J. Phys. Chem. A **2009,** *113,* 11949–11953

The Accuracy of Geometries for Iron Porphyrin Complexes from Density Functional Theory[†]

Patrik Rydberg* and Lars Olsen

Department of Medicinal Chemistry, Copenhagen University, Universitetsparken 2, DK-2100 Copenhagen, Denmark

Received: April 18, 2009; Revised Manuscript Received: June 17, 2009

Iron porphyrin complexes are cofactors in many important proteins such as cytochromes P450, hemoglobin, heme peroxidases, etc. Many computational studies on these systems have been done over the past decade. In this study, the performance of some of the most commonly used density functional theory functionals is evaluated with regard to how they reproduce experimental structures. Seven different functionals (BP86, PBE, PBE0, TPSS, TPSSH, B3LYP, and B97-D) are used to study eight different iron porphyrin complexes. The results show that the TPSSH, PBE0, and TPSS functionals give the best results (absolute bond distance deviations of 0.015−0.016 Å), but the geometries are well-reproduced by all functionals except B3LYP. We also test four different basis sets of double-ζ quality, and we find that a combination of double-ζ basis set of Schäfer et al. on the iron atom and the 6-31G* basis set on the other atoms performs best. Finally, we remove the porphyrin side chains and increase the basis set size systematically to see if this affects the results. We show that basis sets larger than double-ζ quality are not necessary to get accurate geometries, and nonaromatic side chains do not affect the geometries.

Introduction

Iron porphyrin complexes are important cofactors in many enzymes such as cytochromes P450, globins, heme peroxidases, catalases, etc. These enzymes are important for the function of the human body and have thus gathered much interest among researchers for many years. During the past decade, these systems have become accessible to computational studies by the combination of density functional theory (DFT) and increasing computer performance. Today, these systems can even be studied using single CPU computers.

A prerequisite for all computational studies is a reliable structure, before properties such as reaction barriers or spectroscopic data can be determined. While porphyrin molecules have been studied for some time, only a few studies have been made on how DFT reproduces the experimental structures of these systems,[1−3] each study including only one or two axial ligands (imidazole and water or chlorine). In none of these studies have the complete reference systems been used (the porphyrin side chains have always been removed from the crystal structures), and various basis sets have not been compared. Although the geometric performance of DFT for metal-containing structures has been studied comprehensively before,[4,5] no porphyrin systems were included in these studies. Thus, it is still difficult to select the right DFT functional and basis set for these kinds of systems.

In this study, seven functionals are compared to X-ray[6−11] and EXAFS[12,13] data for eight different models with varying ligands binding to the iron atom as shown in Figure 1. These models have been selected to include a variation of axial iron ligands (methylimidazole, pyridine, sulfate, tetrafluorophenylsulfide, and chlorine), distal iron ligands (none, dioxygen, cyanide, phenyl, and oxygen), and iron oxidation states (II, III, and IV).

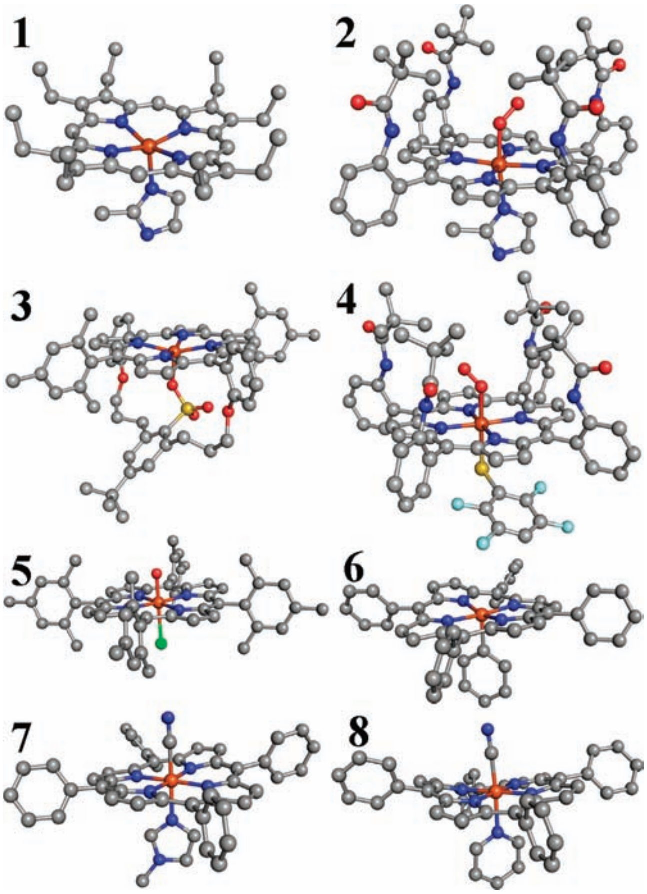

Figure 1. Eight models studied. Hydrogen atoms are not shown due to clarity. Atoms are colored as follows: carbon, gray; nitrogen, blue; oxygen, red; sulfur, yellow; iron, orange; chlorine, green; and fluorine, cyan.

Most of the previous studies on porphyrin systems have been done with basis sets of double or triple-ζ quality on the iron

---

[†] Part of the "Walter Thiel Festschrift".

* To whom correspondence should be addressed. Tel: (+45)35 33 61 62. Fax: (+45)35 30 60 40. E-mail: pry@farma.ku.dk.

10.1021/jp9035716 CCC: $40.75

TABLE 1: Formal Iron Charge, Spin, Number of Atoms, and Basis Functions in the Calculations

					basis functions			
model	ref	iron	spin	atoms	def2-SV(P)	def2-SVP	BS1	LACVP**
1	6	II	quintet	97	768	925	785	916
2	7, 13	II	singlet	155	1340	1557	1357	1548
3	8	III	sextet	138	1214	1404	1231	1395
4	9	II	singlet	155	1404	1606	1421	1597
5	12	IV	quartet	115	1000	1163	1017	1154
6	10	III	doublet	88	846	952	863	943
7	11	III	doublet	91	876	985	893	976
8	11	III	doublet	90	874	980	891	971

atom, and double-ζ quality basis sets on the other atoms. The most commonly used basis set for noniron atoms is 6-31G*, while for the iron atom many different basis sets have been used, for example, the LANL2DZ basis set with effective core potential[14] and the Ahlrichs DZP[15] and VTZ basis sets.[3] To get an understanding of how much the geometry depends on the kind of basis set, we also compare four basis sets and study how porphyrin side chains as well as basis set size affect geometries.

Computational Methodology

The DFT calculations were performed with the Turbomole software, version 5.10.[16] Geometry optimizations were performed using the default settings of the software. All calculations were done using the unrestricted formalism for open shell systems, including the singlets. Similar systems have previously been shown to be more stable as open shell singlets, as compared to closed shell singlets.[17] The open shell singlet is also much more similar to results from CASPT2 calculations[18,19] than the closed shell singlet. Seven different functionals and four different basis sets were used. The functionals were the generalized gradient approximation (GGA) functionals BP86[20,21] and PBE,[22,23] the meta-GGA functional TPSS,[22,24] the hybrid GGA functionals B3LYP[20,25,26] and PBE0,[22,23,27] the hybrid meta-GGA functional TPSSH,[22,24,28] and the GGA functional B97-D with long-range dispersion correction included.[29,30] The basis sets used were a combination previously used by us,[31] which consists of the double-ζ basis set of Schäfer et al.,[32] enhanced with a *p* function with the exponent 0.134915, on the iron atom, and the 6-31G* basis set[33−35] for the other atoms (from here on denoted BS1), two split valence basis sets from Weigend and Ahlrichs (the def2-SV(P) and def2-SVP basis sets),[36] and the LACVP** basis set (the effective core potential basis set LANL2DZ[37] on the iron atom, the 6-31G** basis set[33−35] on hydrogen atoms, and the 6-31G* basis[33−35] on all other atoms).

The size of the complexes varies from 88 to 155 atoms, which for the different basis sets results in 768−1606 basis functions in our calculations as shown in Table 1. The spin states used in the calculations are high- or low-spin as reported in the publications. The spin state of 5 was not reported,[12] but in our calculations, the quartet spin state is lower in energy than the doublet spin state for all of the functional/basis set combinations (see Table S1 in the Supporting Information), and thus, we have used the geometries of the quartet spin state in our evaluations.

All deviations from experimental data have been calculated with the experimental standard deviation subtracted. Thus, any deviation that is less than the reported standard deviation is reported as zero. Deviations are presented as the mean absolute deviation (MAD) and mean deviation (MD) when appropriate. Model 5 has only been used when studying the bond lengths because this is the only data that EXAFS provides.

Bond deviations have been calculated from all bonds including the iron atom. Angle deviations have been calculated from all angles with the iron atom in the center as well as angles with the iron atom at one end and containing ligand atoms (see Tables S2−S33 in the Supporting Information for full lists of bonds and angles). Root mean square deviations (RMSD) of the structure around the iron atom have been calculated in two different manners, first for the iron atom and all of the atoms bound to it ($\mathrm{RMSD}_{\mathrm{FE+1}}$) and second including also the atoms bound to the atoms included in $\mathrm{RMSD}_{\mathrm{FE+1}}$ ($\mathrm{RMSD}_{\mathrm{FE+2}}$). The out-of-plane distance ($\mathrm{Fe}_{\mathrm{oop}}$) from the iron atom to the porphyrin plane has been calculated as the distance from the iron atom to the average plane of the four nitrogen atoms in the porphyrin ring.

Of the seven models for which the DFT optimization started from crystal structure coordinates (models 1−4 and 6−8), only model 3 shows significant changes to the structure. In this crystal structure, the axial SO_3^- ligand is slightly rotated, and the aromatic ring and the SO_3^- ligand are closer to the porphyrin ring than in the optimized structures. This difference is most likely because of packing in the crystal. This can of course affect the comparison of DFT data to crystal data, and thus, comparisons for this model should not be considered to be as accurate as the other models.

Results and Discussion

First, we compare the performance of seven different functionals when used with the BS1 basis set (when not otherwise mentioned), and then, we discuss the results with the other three basis sets.

Bonds. When we compare the bond lengths for the seven DFT functionals, the smallest absolute deviation is given by TPSSH and PBE0 (MAD is 0.015 Å; see Table 2), while PBE0 gives the smallest average deviation (MD is 0.011 Å), and TPSS gives the smallest maximum deviation (MaxD is 0.065 Å),

It is worth noting that PBE0 and TPSSH are the only functionals that give absolute and average errors below or equal to 0.021 Å for each of the eight models (see Tables S2−S33 in the Supporting Information). If we disregard model 3 (as discussed in the Computational Methodology section), TPSS also achieves the same accuracy.

The maximum errors are quite large, ranging from 0.065 to 0.109 Å (TPSS and B3LYP, respectively). However, these are mainly due to the Fe−O_2 bonds in models 2 and 4 and the iron ligand bonds in the two cyanide complexes (models 7 and 8), which all seem to be very hard to describe. If we disregard these four bonds, the maximum errors decrease to 0.034−0.087 Å for TPSS and B3LYP, respectively (see $\mathrm{MaxD}_{\mathrm{alt}}$ in Table 2).

The results in Table 2 show that the B3LYP functional gives both the longest bonds and the largest average bond deviation (see Table 2, column MD). It specifically gives the longest bonds between the iron atom and its axial ligand, on average 0.028 Å longer than the other functionals (see Table S34 in the Supporting Information). B3LYP also results in longer iron−$\mathrm{N}_{\mathrm{por}}$ bonds than the other functionals (0.013 Å longer). The problem with long bonds between the iron and its axial ligand when using the B3LYP functional is similar to that for cobolt in cobalamins,[38] which also have a conjugated ring system with nitrogen atoms bound to the transition metal. Strickland and Harvey also found that the B3LYP functional gives the largest deviations for the bonds to the iron atom using porphyrin complexes;[2] however, they compared model systems to data

TABLE 2: Overview of the Geometric Performance of the Seven Functionals with the Four Different Basis Sets[a]

		bonds				RMSDs		angles
functional	basis set	MAD[b]	MD[c]	MaxD[d]	MaxD$_{alt}$[e]	FE+1[f]	FE+2[g]	MAD[b]
BP	def2-SV(P)	0.020	0.016	0.077	0.043	0.057	0.168	1.67
	def2-SVP	0.020	0.015	0.082	0.042	0.056	0.162	1.63
	LACVP**	0.022	0.017	0.096	0.065	0.054	0.147	1.59
	BS1	0.019	0.014	0.090	0.037	0.055	0.146	1.68
PBE	def2-SV(P)	0.020	0.015	0.075	0.042	0.056	0.173	1.62
	def2-SVP	0.024	0.018	0.078	0.078	0.060	0.161	1.67
	LACVP**	0.022	0.017	0.105	0.064	0.054	0.149	1.60
	BS1	0.019	0.014	0.088	0.039	0.056	0.143	1.67
TPSS	def2-SV(P)	0.017	0.014	0.067	0.039	0.055	0.167	1.68
	def2-SVP	0.017	0.013	0.063	0.037	0.055	0.162	1.68
	LACVP**	0.019	0.015	0.073	0.073	0.056	0.150	1.75
	BS1	0.016	0.012	0.065	0.034	0.055	0.146	1.72
B3LYP	def2-SV(P)	0.028	0.027	0.116	0.047	0.065	0.177	1.68
	def2-SVP	0.029	0.028	0.095	0.077	0.064	0.156	1.65
	LACVP**	0.030	0.029	0.111	0.067	0.068	0.145	1.83
	BS1	0.028	0.028	0.109	0.087	0.064	0.139	1.73
PBE0	def2-SV(P)	0.016	0.009	0.084	0.029	0.056	0.165	1.61
	def2-SVP	0.016	0.012	0.076	0.047	0.056	0.147	1.60
	LACVP**	0.016	0.012	0.051	0.042	0.057	0.145	1.69
	BS1	0.015	0.011	0.066	0.049	0.055	0.139	1.68
TPSSH	def2-SV(P)	0.016	0.013	0.084	0.031	0.056	0.162	1.69
	def2-SVP	0.016	0.013	0.059	0.041	0.055	0.158	1.65
	LACVP**	0.017	0.014	0.086	0.081	0.059	0.165	1.83
	BS1	0.015	0.012	0.085	0.043	0.056	0.140	1.73
B97-D	def2-SV(P)	0.022	0.019	0.106	0.042	0.058	0.161	1.69
	def2-SVP	0.020	0.018	0.113	0.040	0.059	0.161	1.73
	LACVP**	0.022	0.019	0.089	0.038	0.059	0.184	1.84
	BS1	0.019	0.016	0.090	0.036	0.055	0.139	1.71
basis set averages[h]	def2-SV(P)	0.020	0.016	0.116	0.047	0.058	0.167	1.66
	def2-SVP	0.020	0.017	0.113	0.078	0.058	0.158	1.66
	LACVP**	0.021	0.018	0.111	0.081	0.058	0.155	1.74
	BS1	0.019	0.015	0.109	0.087	0.057	0.142	1.70
functional averages[h]	BP	0.020	0.015	0.096	0.065	0.055	0.156	1.64
	PBE	0.021	0.016	0.105	0.078	0.056	0.156	1.64
	TPSS	0.017	0.014	0.073	0.073	0.055	0.156	1.71
	B3LYP	0.029	0.028	0.116	0.087	0.065	0.154	1.72
	PBE0	0.016	0.011	0.084	0.049	0.056	0.149	1.65
	TPSSH	0.016	0.013	0.086	0.081	0.056	0.156	1.73
	B97-D	0.021	0.018	0.113	0.042	0.058	0.161	1.74

[a] Bond deviations and RMSDs in Å, and angle deviations in degrees. [b] Mean absolute deviation. [c] Mean deviation. [d] Maximum deviation. [e] Maximum deviation with the Fe−O_2 bonds excluded. [f] RMSD for the iron atom and all of the atoms bound to it. [g] RMSD for the atoms included in $\text{RMSD}_{\text{FE+1}}$ and the atoms bound to these atoms. [h] Max deviations are not averaged.

from larger complexes. Thus, it seems quite clear that the B3LYP functional is not the one to choose when looking for an accurate description of the bonds to the iron atom. The question is then of course, why do B3LYP result in these long bonds? It is not a result of the HF exchange, because then the PBE0 and TPSSH functionals would also give long bonds (at least as compared to their GGA counterparts, PBE and TPSS). However, calculations on models 6 and 7 using the BLYP functional[20,25] and the BS1 basis set also result in long bonds between the iron atom and the axial ligand (data not shown). This indicates that the LYP correlation[25] is what causes these long bonds (at least when used in combination with double-ζ quality basis sets).

RMSD. We have also studied the RMSD of the iron atom and its surroundings. All functionals except B3LYP give an $\text{RMSD}_{\text{FE+1}}$ of 0.055−0.056 Å (see Table 2). The variations for $\text{RMSD}_{\text{FE+2}}$ are also small, ranging from 0.139 to 0.146 Å. The best results are given by the hybrid functionals and the B97-D functional, which all give $\text{RMSD}_{\text{Fe+2}}$ of 0.139−0.140 Å, while the GGA functionals give slightly larger deviations (0.143−0.146 Å). Thus, according to the two RMSD measurements, PBE0 and B97-D are the best functionals, but even if the B3LYP functional does not reproduce the bonds to the iron atom very well, the overall structure around the iron atom is well reproduced.

Angles. Considering the iron-related angles and as compared to the experimental data, most functionals perform in a similar fashion for all models, except models 1, 3, and 6. For these models, the B97-D functional gives significantly larger, smaller, and smaller deviations, respectively (1.58°, 2.92°, and 1.01°,

TABLE 3: Absolute Deviations in Degrees for Iron-Related Angles in All of the Models Together and Each by Themselves for Each Functional, Computed with the BS1 Basis Set

		model[b]						
functional	total[a]	1	2	3	4	6	7	8
BP	1.68	0.79	2.86	3.68	1.03	1.53	0.95	1.32
PBE	1.67	0.77	2.85	3.63	1.00	1.63	0.98	1.26
TPSS	1.72	0.83	2.85	3.41	1.17	1.64	1.11	1.33
B3LYP	1.73	0.73	2.84	3.42	1.22	1.71	1.09	1.38
PBE0	1.68	0.64	2.82	3.48	1.10	1.73	1.07	1.27
TPSSH	1.73	0.76	2.89	3.43	1.28	1.72	1.14	1.21
B97-D	1.71	1.58	2.93	2.92	1.02	1.01	1.24	1.43

[a] The total is for all of the measured angles in models 1−4 and 6−8; it is not an average of the seven models. [b] Because the reference data for model 5 is from EXAFS measurements, it is not used here.

respectively; see Table 3). This is directly related to the fact that for model 1 the B97-D functional results in a shorter out-of-plane distance for the iron atom to the porphyrin plane as compared to the other functionals, and for models 3 and 6, the porphyrin ring gets a slightly different twist with B97-D as compared to the other functionals.

Increasing the Size of the Basis Sets and the Effect of Porphyrin Side Chains. To investigate if there is a significant effect of the porphyrin side chains as well as the size of the basis sets, we removed the porphyrin side chains of models 1 and 2 and optimized the geometry using the TPSS functional[22,24] (the best nonhybrid functional as shown above) and the def2-SVP basis set.[36] Without side chains, we also optimized the geometries with the def2-TZVP and def2-QZVP basis sets.[36] The most important geometric measures are shown in Table 4. It has previously been shown that the side chains of porphyrin IX have very little effect on the geometry,[39] and this is also the case for the even simpler side chains of model 1. While the bond lengths are almost identical with and without side chains, there are some differences that can be seen in RMSDs and angles. These are due to a 14° change in the rotation of the methylimidazole ligand (the same rotation changes slightly also with the TZVP and QZVP basis sets, 11.4° and 5.9°, respectively). For model 2, however, there are clear changes in the bond lengths when we remove the side chains. The bonds from the iron atom to the porphyrin nitrogen atoms as well as the methyl-imidazole nitrogen atom become longer (0.01 and 0.02 Å, respectively). However, for the RMSDs and the angles, the changes are small. Because the geometry around the iron atom does not change significantly when removing the side chains for model 1, it is quite clear that for geometries, porphyrin models with simple side chains (e.g., alkyl and vinyl groups) can be studied without side chains to high accuracy, but for porphyrin models with aromatic side chains, this is not necessarily true.

When comparing the double-ζ geometry (SVP) with the results from the larger basis sets (triple and quadruple-ζ), is not clear if the triple and quadruple-ζ basis gives better geometry than the doublet ζ basis. Thus, the large increase in basis functions using the triple-ζ and quadruple-ζ basis sets is unnecessary when computing geometries for porphyrin complexes.

Other Basis Sets of Double-ζ Quality. The bonds to the iron atom are best reproduced by the BS1 basis set (on average, MAD is 0.019 Å, and MD is 0.015 Å). The LACVP**, def2-SV(P), and the def2-SVP basis sets give slightly longer bond lengths and slightly larger absolute deviations (see Table 2); however, the differences are small.

When comparing the RMSDs for the for the four basis sets, it is clear that the BS1 basis set gives the most consistent results, always giving the lowest RMSD$_{FE+2}$, and also the lowest, or within 0.001 Å of the lowest, RMSD$_{FE+1}$ for all functionals except PBE (where it is within 0.002 Å of the lowest). On average, the trends are the same as for the bond lengths.

The LACVP** basis set results in both the largest and the smallest absolute deviations for the angles. In combination with the BP and PBE functionals, it gives the smallest deviations (1.58−1.59°), while in combination with B3LYP, TPSSH, and B97-D, it gives the largest deviations (1.83−1.84°). This is a result of an uneven performance on the different models, especially models 1 (where it is worse than the other basis sets) and 6 (where it is better than the other basis sets in combination with the BP and PBE functionals). It is also worth noting that the LACVP** basis set always gives the longest bond from the iron atom to the axial ligand in the three models with oxygen bound to the iron atom (models 2, 4, and 5).

Conclusions

We have evaluated the performance of seven functionals and four basis sets for the geometry of eight iron porphyrin complexes. The results show that the TPSSH and PBE0 functionals are slightly better than the BP, PBE, TPSS, and B97-D functionals, which in turn are significantly better than B3LYP.

While the B3LYP functional has been used for many studies of porphyrin complexes, our results together with a previous study by Strickland[2] show that this functional should not be used for accurate geometries of iron porphyrins.

TABLE 4: Iron−Ligand, Iron−Oxygen, and Average Iron−Porphyrin Nitrogen Distances in Ångstroms, the RMSDs, and Absolute Deviations of Angles for Models 1 and 2 with and without Side Chains from Calculations Performed with the TPSS Functional

	model 1					model 2				
	exp.[a]	full[b]	small[c]			exp.[a]	full[b]	small[c]		
basis set		SVP	SVP	TZVP	QZVP		SVP	SVP	TZVP	QZVP
basis functions		925	541	1083	2334		1557	569	1145	2448
Fe−N$_{pyr}$	2.077	2.091	2.092	2.083	2.080	1.996	1.997	2.006	2.003	1.998
Fe−N$_{lig}$	2.135	2.167	2.166	2.177	2.170	2.107	2.110	2.131	2.145	2.120
Fe−O						1.898	1.836	1.832	1.830	1.826
RMSD$_{FE+1}$		0.031	0.023	0.027	0.030		0.078	0.076	0.075	0.076
RMSD$_{FE+2}$		0.101	0.163	0.145	0.118		0.225	0.203	0.188	0.185
MAD angles		0.80	0.47	0.64	0.72		2.83	2.94	2.89	2.91

[a] Experimental data from crystal structures. [b] The full model used in our comparisons above. [c] Model with the porphyrin side chains removed.

With regard to the basis sets, the results show that the BS1 basis set combination gives the most consistent results for bonds and RMSDs. Combining the BS1 basis set with either of the BP, PBE, PBE0, TPSS, TPSSH, or B97-D functionals will almost always give good geometries. Adding our results to previous work on geometries,[4] as well as heats of formation and ionization potentials for transition metal systems,[40] it seems that for systems containing transition metals the TPSS functional is one of the best to use.

From a practical point of view, we find that the scf calculations are much easier to converge with the hybrid GGA functionals, B3LYP and PBE0, and the hybrid meta-GGA functional TPSSH. However, the BP, PBE, and TPSS functionals can be used in conjunction with the resolution of identity approach,[41,42] which speeds up the calculations significantly.

For iron porphyrin complexes with nonaromatic side chains, one can remove the side chains without affecting the geometry around the iron atom. However, for complexes with aromatic side chains, there are clear effects on the length of the bonds to the iron atom when the side chains are removed. Our systematic investigation of basis set size using the def2 basis sets of Ahlrichs[36] shows that a double-ζ basis is large enough to get accurate geometries for porphyrin complexes with DFT.

Acknowledgment. We thank Jean Fischer (retired, previously Université Luis Pasteur) and Louis Picard of École Polytechnique for supplying the crystal structure of model 4. This work was supported by grants from the Benzon Foundation and the Danish medical research council.

Supporting Information Available: Iron−ligand distances, iron−oxygen distances, iron-related angles, and doublet and quartet spin state energies of model 5. This material is available free of charge via the Internet at http://pubs.acs.org.

References and Notes

(1) Ghosh, A.; Vangberg, T.; Gonzalez, E.; Taylor, P. *J. Porphyrins Phthalocyanines* **2001**, *5*, 345–356.

(2) Strickland, N.; Harvey, J. N. *J. Phys. Chem. B* **2007**, *111*, 841–852.

(3) Smith, D. M. A.; Dupuis, M.; Straatsma, T. P. *Mol. Phys.* **2005**, *103*, 273–278.

(4) Buhl, M.; Kabrede, H. *J. Chem. Theory Comput.* **2006**, *2*, 1282–1290.

(5) Hamprecht, F. A.; Cohen, A. J.; Tozer, D. J.; Handy, N. C. *J. Chem. Phys.* **1998**, *109*, 6264–6271.

(6) Hu, C. J.; An, J.; Noll, B. C.; Schulz, C. E.; Scheidt, W. R. *Inorg. Chem.* **2006**, *45*, 4177–4185.

(7) Jameson, G. B.; Molinaro, F. S.; Ibers, J. A.; Collman, J. P.; Brauman, J. I.; Rose, E.; Suslick, K. S. *J. Am. Chem. Soc.* **1980**, *102*, 3224–3237.

(8) Meyer, D.; Leifels, T.; Sbaragli, L.; Woggon, W. D. *Biochem. Biophys. Res. Commun.* **2005**, *338*, 372–377.

(9) Schappacher, M.; Ricard, L.; Fischer, J.; Weiss, R.; Bill, E.; Montielmontoya, R.; Winkler, H.; Trautwein, A. X. *Eur. J. Biochem.* **1987**, *168*, 419–429.

(10) Doppelt, P. *Inorg. Chem.* **1984**, *23*, 4009–4011.

(11) Li, J. F.; Noll, B. C.; Schulz, C. E.; Scheidt, W. R. *Inorg. Chem.* **2007**, *46*, 2286–2298.

(12) Wolter, T.; Meyer-Klaucke, W.; Muther, M.; Mandon, D.; Winkler, H.; Trautwein, A. X.; Weiss, R. *J. Inorg. Biochem.* **2000**, *78*, 117–122.

(13) Woolery, G. L.; Walters, M. A.; Suslick, K. S.; Powers, L. S.; Spiro, T. G. *J. Am. Chem. Soc.* **1985**, *107*, 2370–2373.

(14) Shaik, S.; Kumar, D.; de Visser, S. P.; Altun, A.; Thiel, W. *Chem. Rev.* **2005**, *105*, 2279–2328.

(15) Rydberg, P.; Ryde, U.; Olsen, L. *J. Phys. Chem. A* **2008**, *112*, 13058–13065.

(16) Ahlrichs, R.; Bar, M.; Haser, M.; Horn, H.; Kolmel, C. *Chem. Phys. Lett.* **1989**, *162*, 165–169.

(17) Rydberg, P.; Sigfridsson, E.; Ryde, U. *J. Biol. Inorg. Chem.* **2004**, *9*, 203–223.

(18) Jensen, K. P.; Roos, B. O.; Ryde, U. *J. Inorg. Biochem.* **2005**, *99*, 45–54.

(19) Jensen, K. P.; Roos, B. O.; Ryde, U. *J. Inorg. Biochem.* **2005**, *99*, 978.

(20) Becke, A. D. *Phys. Rev. A* **1988**, *38*, 3098–3100.

(21) Perdew, J. P. *Phys. Rev. B* **1986**, *33*, 8822–8824.

(22) Perdew, J. P.; Wang, Y. *Phys. Rev. B* **1992**, *45*, 13244–13249.

(23) Perdew, J. P.; Burke, K.; Ernzerhof, M. *Phys. Rev. Lett.* **1996**, *77*, 3865–3868.

(24) Tao, J. M.; Perdew, J. P.; Staroverov, V. N.; Scuseria, G. E. *Phys. Rev. Lett.* **2003**, 91.

(25) Lee, C. T.; Yang, W. T.; Parr, R. G. *Phys. Rev. B* **1988**, *37*, 785–789.

(26) Becke, A. D. *J. Chem. Phys.* **1993**, *98*, 5648–5652.

(27) Perdew, J. P.; Emzerhof, M.; Burke, K. *J. Chem. Phys.* **1996**, *105*, 9982–9985.

(28) Staroverov, V. N.; Scuseria, G. E.; Tao, J. M.; Perdew, J. P. *J. Chem. Phys.* **2003**, *119*, 12129–12137.

(29) Becke, A. D. *J. Chem. Phys.* **1997**, *107*, 8554–8560.

(30) Grimme, S. *J. Comput. Chem.* **2006**, *27*, 1787–1799.

(31) Olsen, L.; Rydberg, P.; Rod, T. H.; Ryde, U. *J. Med. Chem.* **2006**, *49*, 6489–6499.

(32) Schafer, A.; Horn, H.; Ahlrichs, R. *J. Chem. Phys.* **1992**, *97*, 2571–2577.

(33) Hehre, W. J.; Ditchfield, R.; Pople, J. A. *J. Chem. Phys.* **1972**, *56*, 2257–2261.

(34) Hariharan, P. C.; Pople, J. A. *Theor. Chim. Acta* **1973**, *28*, 213–222.

(35) Francl, M. M.; Pietro, W. J.; Hehre, W. J.; Binkley, J. S.; Gordon, M. S.; Defrees, D. J.; Pople, J. A. *J. Chem. Phys.* **1982**, *77*, 3654–3665.

(36) Weigend, F.; Ahlrichs, R. *Phys. Chem. Chem. Phys.* **2005**, *7*, 3297–3305.

(37) Hay, P. J.; Wadt, W. R. *J. Chem. Phys.* **1985**, *82*, 299–310.

(38) Jensen, K. P.; Ryde, U. *J. Phys. Chem. A* **2003**, *107*, 7539–7545.

(39) Sigfridsson, E.; Ryde, U. *J. Biol. Inorg. Chem.* **2003**, *8*, 273–282.

(40) Riley, K. E.; Merz, K. M. *J. Phys. Chem. A* **2007**, *111*, 6044–6053.

(41) Eichkorn, K.; Treutler, O.; Ohm, H.; Haser, M.; Ahlrichs, R. *Chem. Phys. Lett.* **1995**, *242*, 652–660.

(42) Eichkorn, K.; Treutler, O.; Ohm, H.; Haser, M.; Ahlrichs, R. *Chem. Phys. Lett.* **1995**, *240*, 283–289.

JP9035716